



Design M×N Adaptive Antenna Array for Personal - Satellite Communications Link

Mabrouka H. A. Ehtaiba and Hend M. Elamari

Department of Electrical and Electronic Engineering, Faculty of Engineering, Sirte University, Sirte, Libya.

© SUSJ2023.

DOI: <https://doi.org/10.37375/susj.v13i1.1367>

A B S T R A C T

ARTICLE INFO:

Received 13 December 2022.

Accepted 10 March 2023.

Available online 01 June 2023.

Keywords: Adaptive planner antenna, Radiation pattern, Satellite mobile communication.

This paper introduces a proposed design of an adaptive rectangular microstrip antenna array for personal - satellite communications link operating at 3 GHz. The main purpose is to design an antenna with an adaptive narrow main beam bandwidth directing up to the satellite by using smart antenna techniques. The performance of the proposed planer antenna in terms of patch width and length, number of elements along the x-axis and y-axis, the spacing between the elements, directivity, distribution, weighting coefficients, and radiation pattern are studied and optimized using Matlab software. High directivity of 13.12 dB is achieved. Therefore, high orbits satellites cab be utilized to reduce the cost.

1 Introduction

In the recent years of development in communication systems a need for the development of compact, lightweight, and cost-effective antennas that are capable of maintaining high performance over a wide range of frequencies. This technological trend has focused much effort on the design of a microstrip patch antenna with adaptive techniques called smart antenna (Luo & Gao, 2014). These techniques achieve a great increase in the performance of mobile cellular communications systems by improving immunity to co-channel interference. As it is known, there are some regions that cannot be covered by the cellular system like ocean, desert, forests, and remote rural regions, because of building base stations in such areas is very expensive. In this instance, mobile satellite communications are a powerful solution to overcome this limitation, where the mobile directly contacts the satellite through space. A satellite simply orbits around the orbit, any object that revolves around a planet in a circular or elliptical path (Rappaport, 2002). The mobile satellite communication systems can be classified in terms of satellite orbits into, static orbit systems and non-static orbit systems (synchronous and asynchronous orbit).

Geostationary Earth Orbit (GEO) falls under the static and because of its distance (35800km) to the ground; it is very unfavorable to communicate with personal terminals on ground directly, so most mobile satellite communication systems are all adopted non-static orbits at present (Abo-Zeed, Din, Shayea, & Ergen, 2019). The non-static orbit satellites have two big classes, which are circular orbits and oval orbits. Oval orbits like Highly Elliptical Orbit (HEO) are good for regional coverage, but the angle of inclination of the orbit planes must be put to consideration, it is must be 63.14° (Wu & Li, 2005), this is a disadvantage for coverage of locations with lower latitude. The angle of inclination of circular orbit planes can be set between 0° and 90° at random.

Circular orbits mobile satellite communication systems are divided into medium earth orbit (MEO), lower earth orbit (LEO), and geostationary orbit (GEO) as described in Table 1. GEO is about 35800 Km above the equator, the delay and losses are greater, but the advantages are more coverage (it covers 40% of the earth) and there no need to track the satellite.

Table 1: Types of circular orbits.

Parameter	LEO	MEO	GEO
Satellite height	500-1500 km	5000-12000 km	35,800km
Orbital Period	10-40 minutes	2-8 hours	24 hours
Satellites No.	40-80	8-20	3
Satellite Life	short	Long	Long
Handoffs No.	High	Low	Least(none)
Propagation Loss	Least	High	Highest

As the altitude of a satellite increases on earth, the total required satellites number and cost decrease. Although of these advantages, another factor can be affected the signal strength incredibly, as distance increases, that is free space loss (FSL). In telecommunication, free-space path loss (FSPL) is the loss in signal strength of an electromagnetic wave that would result from a line-of-sight path through free space (usually air), with no obstacles nearby to cause reflection or diffraction (Karaliopoulos & Pavlidou, 1999). FSPL is proportional to the square of the distance between the transmitter and receiver, and proportional to the square of the frequency of the radio signal. Signal disperses with distance. This form of attenuation expresses in terms of the ratio of the radiated power to the power received by the antenna. For the ideal isotropic antenna, FSPL is given by (Karaliopoulos & Pavlidou, 1999) as expressed in Eq. (1):

$$\frac{P_t}{P_r} = \frac{(4 \pi Y)^2}{\lambda^2} = \frac{(4 \pi f Y)^2}{c^2} \quad (1)$$

where: λ is the signal wavelength (in metres), f is the signal frequency (in hertz), Y is the distance from the satellite (in metres), c is the speed of light in a vacuum. This equation is only accurate in the far field where spherical spreading can be assumed; it does not hold close to the satellite. If the used frequency is 3 GHz, $\lambda=10$ cm, $Y=1000$ km then, $FSL=162$ dB. But if orbit radius $Y=5000$ km, then $FSL=176$ dB. The signal is attenuated by 14 dB. Therefore, in this research, an antenna with high gain to compensate the attenuation of signal intensity without increasing the transmitted power will be designed. Thus, by achieving this, high orbits satellites can be utilized to reduce the cost.

2 Antenna Design

The rapid development in communications requires the development of low cost, minimal weight, and low-profile antennas that are capable of maintaining high performance as a result of development of integrated circuits "IC". The Mono-pole antenna that used in the mobile is undesired in terms of design due to its size compared with phone body. In addition, its gain is small that resulting in increasing the radiated power. Microstrip patch antennas are the most widely used

types of antennas in the microwave frequency range (Garg, 2001). A microstrip antenna consists of conducting patch on a ground plane separated by dielectric substrate of certain thickness h and a dielectric constant ϵ_r as shown in Figure 1.

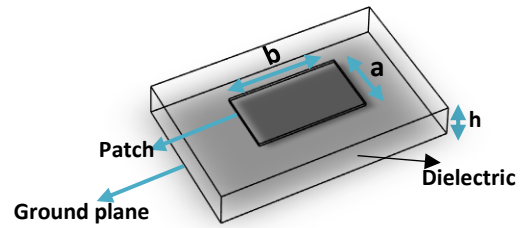


Figure 1: Microstrip antenna.

In order to simplify analysis and performance predication, the patch is generally square, rectangular, circular, triangular, and elliptical or some other common shape. For a rectangular patch, the length a of the patch is usually $0.3333\lambda_0 < a < 0.5\lambda_0$ where λ_0 is the free-space wavelength. The patch is selected to be very thin such that $t \ll \lambda_0$ (where t is the patch thickness). The height h of the dielectric substrate is usually $0.003\lambda_0 \leq h \leq 0.05\lambda_0$. Microstrip patch antennas radiate primarily because of the fringing fields between the patch edge and the ground plane. For good antenna performance, a thick dielectric substrate having a low dielectric constant is desirable since this provides better efficiency, larger bandwidth and better radiation (Behera, 2007). However, such a configuration leads to a larger antenna size. In order to design a compact microstrip patch antenna, substrates with higher dielectric constants must be used which are less efficient and result in narrower bandwidth. Hence a trade-off must be realized between the antenna dimensions and antenna performance (Kasabegoudar & Kumar, 2013). In this paper, the design of a planner adaptive microstrip antenna array its size is suitable with the mobile satellite size, has been analysed and studied at 3 GHz. Two essential parameters for the design of a rectangular microstrip patch antenna are operation frequency and dielectric substrate height was selected to be ($h=0.025$).

2.1 Radiation pattern of single element

Consider a single element microstrip antenna as shown in Figure (2).

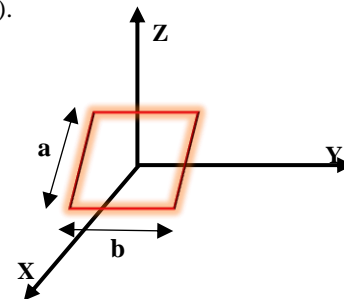


Figure 2: A single element along y-axis.

The single element radiation pattern in electric field plane (E-plane X-Z) and magnetic field plane (H-plane Y-Z) is computed by using Eq.(2) and Eq.(3) respectively (Chrisman, 1989; Yang, Huang, & Hong, 2014):

$$E_{\theta E} = K_T \frac{\sin(k_0 h \sin\theta)}{k_0 h \sin\theta} \cos(k_0 a \sin\theta) \quad (2)$$

$$E_{\theta H} = K_T \frac{\sin(k_0 b \sin\theta)}{k_0 b \sin\theta} \cos\theta \quad (3)$$

$$K_T = -j b k_0 \frac{e^{-j k_0 r}}{4 \pi r} \quad (4)$$

where: h is height of dielectric substrate, b is patch width, a is patch length, k_0 is the propagation constant in free space, V_0 is feed voltage of the antenna.

2.2 The array factor of two-dimensional planar array

Now, it can consider the case where M-elements are placed on straight line i.e., x-axis and separated by the same distance dx, leading to a linear array of total length $D = (M-1) dx$. More development can be obtained by arranging the elements to form a planar array as illustrated in Figure 3. Planar arrays are more versatile; they provide more symmetrical patterns with lower side lobes, much higher directivity (narrow main beam). They can be used to scan the main beam toward any point in space (Chrisman, 1989; Yang et al., 2014):

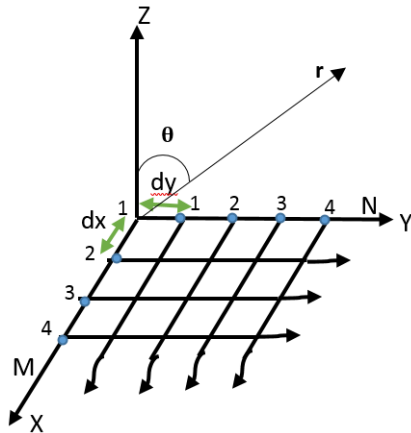


Figure 3: The array factor of a rectangular planar array.

The AF of a linear array of M elements along the x-axis can be written as expressed in Eq. (5):

$$AF = \sum_{m=1}^M W_{m1} e^{j(m-1)(k dx \sin\theta \cos\phi)} \quad (5)$$

where W_{m1} presents weight coefficient when the array in receiving case. $\sin\theta \cos\phi = x$ is the directional cosine with respect to the x-axis. W_{m1} denotes the excitation

amplitude of the element at the point with coordinates: $D = (m-1) dx, y = 0$.

In the Figure (3), this is the element of the m-th row and the 1st column of the array matrix. If N such arrays are placed next to each other in the y direction, a rectangular array will be formed. We shall assume again that they are equispaced at a distance of dy and there is a progressive phase shift along each row of β_y . It will be also assumed that the normalized current distribution along each of the x-directed array is the same, but the absolute values correspond to a factor of W_{1n} ($n=1, \dots, N$). Then, the AF of the entire array will be as expressed in Eq. (6).

$$AF = \sum_{n=1}^N w_{1n} \left[\sum_{m=1}^M w_{m1} e^{j(m-1)(k dx \sin\theta \cos\phi)} \right] e^{j(n-1)(k dy \sin\theta \cos\phi)} \quad (6)$$

or

$$AF = S_{XM} \cdot S_{YN} \quad (7)$$

$$S_{XM} = AF = \sum_{m=1}^M w_{m1} e^{j(m-1)(k dx \sin\theta \cos\phi)} \quad (8)$$

and

$$S_{YN} = AF = \sum_{n=1}^N w_{n1} e^{j(n-1)(k dy \sin\theta \cos\phi)} \quad (9)$$

The pattern of a rectangular array is the product of the array factors of the linear arrays in the x and y directions. For a uniform planar (rectangular) array $w_{m1} = w_{n1} = w_0$, for all m and n, i.e., all elements have the same excitation amplitudes.

$$AF = w_0 \sum_{m=1}^M w_{m1} e^{j(m-1)(k dx \sin\theta \cos\phi)} \sum_{n=1}^N w_{n1} e^{j(n-1)(k dy \sin\theta \cos\phi)} \quad (10)$$

The normalized array factor can be obtained as:

$$AF_n(\theta, \phi) = \left\{ \frac{1}{M} \frac{\sin\left(\frac{M\psi_x}{2}\right)}{\sin\left(\frac{\psi_x}{2}\right)} \right\} \left\{ \frac{1}{N} \frac{\sin\left(\frac{N\psi_y}{2}\right)}{\sin\left(\frac{\psi_y}{2}\right)} \right\} \quad (11)$$

where:

$$\psi_x = k d_x \sin\theta \cos\phi + \beta_x \quad (12)$$

$$\psi_y = k d_y \sin\theta \sin\phi + \beta_y$$

The major lobe (principal maximum) and grating lobes of the terms:

$$S_{xM} = \left\{ \frac{1}{M} \frac{\sin\left(M \frac{\psi_x}{2}\right)}{\sin\left(\frac{\psi_x}{2}\right)} \right\} \quad (13)$$

$$S_{yN} = \left\{ \frac{1}{N} \frac{\sin\left(N \frac{\psi_y}{2}\right)}{\sin\left(\frac{\psi_y}{2}\right)} \right\} \quad (14)$$

are located at angles such that:

$$Kd_x \sin \theta_m \cos \phi_m + \beta_x = \pm 2m\pi, \quad m = 0,1, \dots$$

$$Kd_y \sin \theta_n \cos \phi_n + \beta_y = \pm 2n\pi, \quad n = 0,1, \dots$$

The principal maxima correspond to $m = zero, n = zero$.

In general, β_x and β_y are independent from each other. But, if it is required that the main beams of S_{yN} and S_{xM} intersect (which is usually the case), then the common main beam is in the direction $\theta = \theta_0$ and $\phi = \phi_0, m = n = 0$. If the principal maximum is specified by (ϕ_0, θ_0) , then the progressive phases β_x and β_y must satisfy:

$$\beta_x = -Kd_x \sin \theta_0 \cos \phi_0 \quad (15)$$

$$\beta_y = -Kd_y \sin \theta_0 \sin \phi_0$$

The Eq. (11) was programmed by MATLAB to study the effect of element number and distance on the array factor. The results are presented in section 3.

2.3 The radiation pattern of a two-dimensional array of microstrip antennas and directivity

$$E_{\theta E} = K_T \frac{\sin(k_0 h \sin \theta)}{k_0 h \sin \theta} \cos(k_0 a \sin \theta) \quad (16)$$

$$E_{\theta H} = K_T \frac{\sin(k_0 b \sin \theta)}{k_0 b \sin \theta} \cos(\theta) \quad (17)$$

$$AF_n(\theta, \phi) = \left\{ \frac{1}{M} \frac{\sin\left(M \frac{\psi_x}{2}\right)}{\sin\left(\frac{\psi_x}{2}\right)} \right\} \left\{ \frac{1}{N} \frac{\sin\left(N \frac{\psi_y}{2}\right)}{\sin\left(\frac{\psi_y}{2}\right)} \right\} \quad (18)$$

$$AF_{E-PLAN} = E_{\theta E} * AF_n(\theta, \phi) \quad (19)$$

$$AF_{H-PLAN} = E_{\theta H} * AF_n(\theta, \phi) \quad (20)$$

$$D = \frac{(72815)}{(\theta 1^2 + \theta 2^2)} \quad (21)$$

$$D_o(dB) = 10 \log(D_o) \quad (22)$$

Where: $\theta 1$ is angle of mean beam E-plane, $\theta 2$ is angle of mean beam H-plane, D is directivity, D_o is directivity in dB.

2.4 Steering the antenna main beam

Due to the narrow main beam and the motion of satellite related to mobile station, it is extremely important to steering the narrow main beam width towards satellite, and null value towards interference directions to increase the signal to noise ratio. The antenna array provides the capability of performing the antenna pattern meeting the environment requirement under study.

Adaptive antenna arrays are often called smart antennas because they have some key benefits over traditional antennas, by adjusting traffic patterns, space diversity or using multiple access techniques. The main four key benefits are: firstly, enhanced coverage through range extension by increasing the gain and steering capability of the ground station antenna; secondly, enhanced signal quality through multi-target capability and reduction of interferences; finally, adaptive antennas improve the data download capacity in the ground segment of satellite communication by increasing the coverage range (Rodríguez-Osorio & Natera, 2010). In this section, the used techniques for steering the main beam and null in specific directions will be presented. Let's apply this technique on linear array first and then on planner. Assuming linear array with number of isotropic elements N as illustrated in Figure (4).

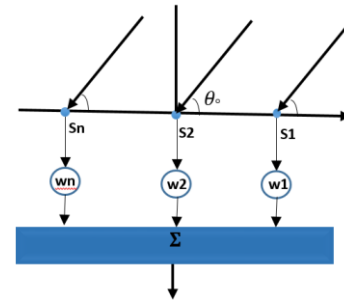


Figure 4: Adaptive antenna system

A linear beam former combines signals according to some weights w_n , to produce a desired radiation pattern. The mathematical expression of a linear beam former at the array output in vector notation can be expressed as $Y = w^t s$, where s is the received signal vector to be combined, w are the weights computed by the beam forming algorithm and t denotes transposition and conjugate of $(.)$ (Rodríguez-Osorio & Natera, 2010). To steer the main beam in desired direction, the out signal from element m is (Chrisman, 1989; Yang et al., 2014):

$$S_m = 1 e^{-j(m-1) kd \cos \theta_0} \tag{23}$$

By multiplying each signal in the w_m , the summation:

$$Y = \sum_{m=1}^N w_m S_m \tag{24}$$

To find out the radiation pattern of the array antenna, changing θ° and each time calculating the out-signal density. The radiation pattern is:

$$Y = \sum_{m=1}^N w_m e^{-j(m-1) kd \cos \theta_0} \tag{25}$$

$$w_m = S_m^* \tag{26}$$

Now, steering the null value in undesired direction: The null steering in antenna radiation pattern of a linear array to reject unwanted interference sources while receiving the desired signal from a chosen direction has attracted considerable attention in the past and still of great interest, the increasing noise and interference pollution of the electromagnetic environment has prompted to study an array pattern nulling techniques. Null steering in phased and adaptive arrays may be achieved by controlling some array parameters such as the complex element weights, element phases, amplitudes, and element positions (Khan & Tuzlukov, 2010). To steering null value in undesired signal (Chrisman, 1989; Yang et al., 2014):

$$Y = \sum_{m=1}^N w_m S_m \tag{27}$$

$$S_m = 1 e^{-j(m-1) kd \cos \theta_0} \tag{28}$$

$$Y = S^t w \tag{29}$$

To make $y=0$, $w \perp S$ is as shown in Figure 5:

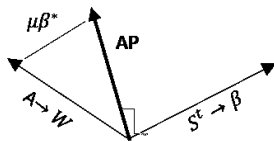


Figure 5: $y=0$, $w \perp S$

$$B^t (A + \mu B^*) = 0 \tag{30}$$

$$B^t A + \mu B^t B^* = 0 \tag{31}$$

$$\mu = -\frac{B^t A}{B^t B^*} \tag{32}$$

$$AP = A + \mu B^* = A + B^* \mu \tag{33}$$

$$AP = A - \frac{B^t A B^*}{B^t B^*} = \left[I - \frac{B^* B^t}{B^t B^*} \right] A \tag{34}$$

$$Y = w^t S \tag{35}$$

$$W_p = \left[I - \frac{S^* S^t}{S^t S^*} \right] w \tag{36}$$

$$Y = W_p^t S \tag{37}$$

The Eq. (37) was programmed by MATLAB to steer the null value in undesired direction, the results are presented in the next section.

Now, steering the main beam and null value in the same moment. (Chrisman, 1989; Yang et al., 2014):

$$S_n = e^{-j(n-1) kd \cos \theta_{0n}} \tag{38}$$

$$S_m = e^{-j(n-1) kd \cos \theta_{0m}} \tag{39}$$

$$W = S_m^* \tag{40}$$

Then, readjust W value:

$$W_p = \left[I - \frac{S^* S^t}{S^t S^*} \right] w \tag{41}$$

The total radiation pattern is:

$$S = e^{-j(n-1) kd \cos \theta_0} \tag{42}$$

$$Y = S * W_p \tag{43}$$

The Eq. (43) was programmed by MATLAB to steer the main beam and null value, the results are presented in the next section.

Steering the main beam and null value of the proposed planner array. In this section, the steering technique that described above will be applied here on a planner array as follows: The array factor of planner array for a signal in direction (θ_0, ϕ_0) can be written as:

$$S_{mnd} = e^{-jk dx (m-1) \sin \theta_0 \cos \phi_0} e^{-jk dy (n-1) \sin \theta_0 \sin \phi_0} \tag{44}$$

To steer the array main beam in the desired direction (θ_o, ϕ_o) , the weighting coefficients must be chosen to satisfy the following condition:

$$W_{mn} = S_{mnd}^* \tag{45}$$

Then, the radiation pattern is:

$$Y(\theta, \phi) = \sum_{m=1}^M \sum_{n=1}^N W_{mn} e^{-jk dx (m-1) \sin \theta_o \cos \phi_o} e^{-jk dy (n-1) \sin \theta_o \sin \phi_o} \tag{46}$$

If there are interference source issuing from the undesired direction of (θ_I, ϕ_I) , then, the array factor becomes:

$$S_{mnl} = e^{-jk dx (m-1) \sin \theta_I \cos \phi_I} e^{-jk dy (n-1) \sin \theta_I \sin \phi_I} \tag{47}$$

To steer null value in the interference direction (θ_I, ϕ_I) , the weighting coefficients must be chosen to satisfy the following condition:

$$W_p = W - \frac{S_I^* S_I^t}{S_I^t S_I^*} * W \tag{48}$$

The final radiation pattern of the array is as given in Eq. (46) with exchanging W by W_p . The Eq. (46) was programmed by using MATLAB and plotted in 3-D and the next figures illustrate steering the main beam and null value in the desired directions.

3 Results

As presented in section 2.1, the Eq. (2) and Eq. (3) were programmed by using MATLAB to compute and plot the radiation pattern in electric field plane (E-plane) and magnetic field plane (H-plane) for single element with different values of the width 'b' and the length 'a' as illustrated in Figures (6) and (7) respectively.

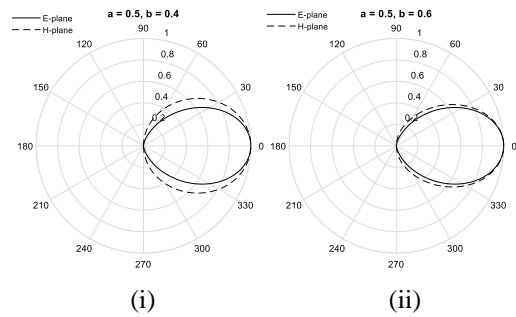


Figure 6: Radiation pattern of single element in E and H planes, (i) a=0.5, b=0.4, (ii) a=0.5, b=0.6

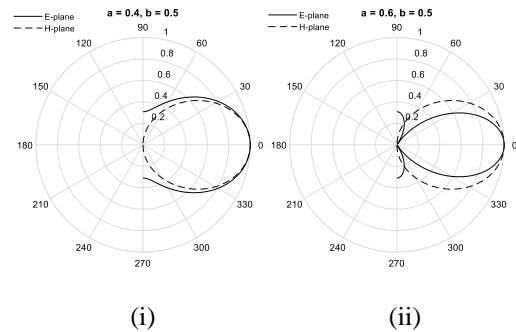


Figure 7: Radiation pattern of single element in E and H planes, (i) a=0.4, b=0.5, (ii) a=0.6, b=0.5

Now, for array antenna has number of elements, the Eq. (11) was programmed by MATLAB to study the effect of elements number and elements distance on the array factor of two-dimensional planner array (PHI angle takes any value, in this case = 90°) as presented in section 2.2. The radiation pattern of planner array antenna due to change of dx and dy is shown in Figures (8-10). The radiation pattern of planner array antenna due to change a N, M is illustrated in Figures (11-13).

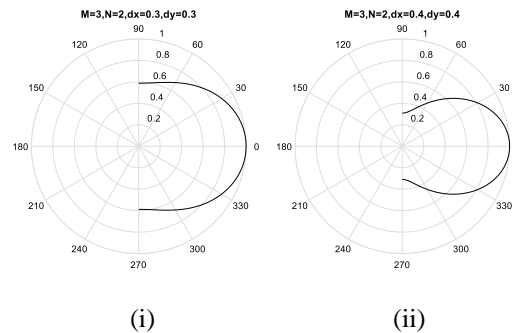


Figure 8: Radiation pattern when the element distance (i) dx=dy=0.3 increases to (ii) dx=dy=0.4

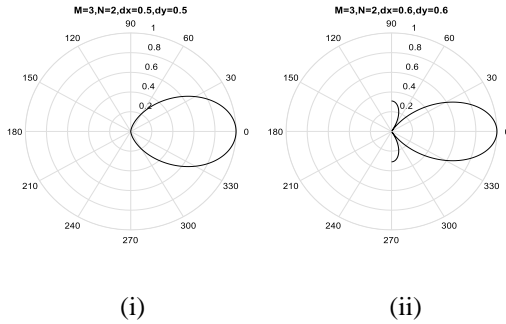


Figure 9: Radiation pattern when the element distance (i) $dx=dy=0.5$ increases to (ii) $dx=dy=0.6$

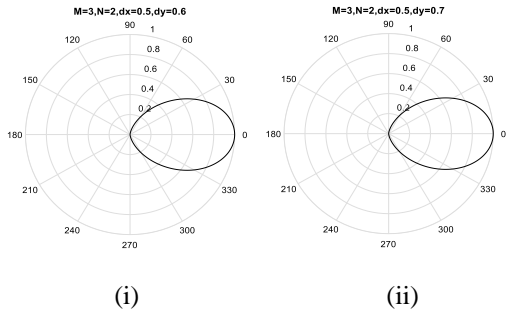


Figure 10: Radiation pattern when the element distance $dx=0.5$ and (i) $dy=0.6$ increases to (ii) $dy=0.7$

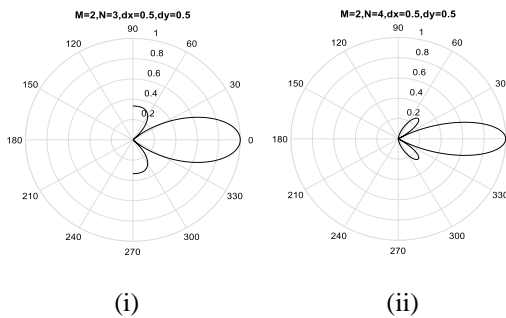


Figure 11: Radiation pattern when the elements number $M=2$ & (i) $N=3$ increases to (ii) $N=4$

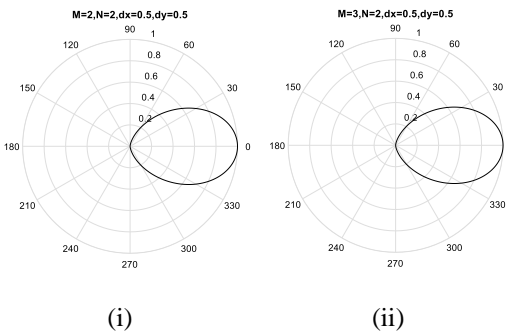


Figure 12: Radiation pattern when the elements number $N=2$ & (i) $M=2$ increases to (ii) $M=3$

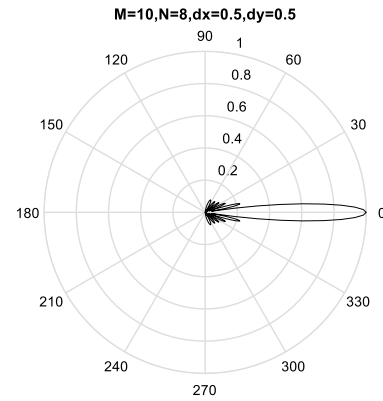


Figure 13: Radiation pattern with large elements number, $M=10$ & $N=8$.

In section 2.3, the radiation pattern of a two-dimensional array of microstrip antennas and directivity was presented. The Eqs. (19-21) were programmed by MATLAB to compute and plot the radiation pattern in E and H planes, then calculate the directivity at different dx and dy values as shown in Figure (14).

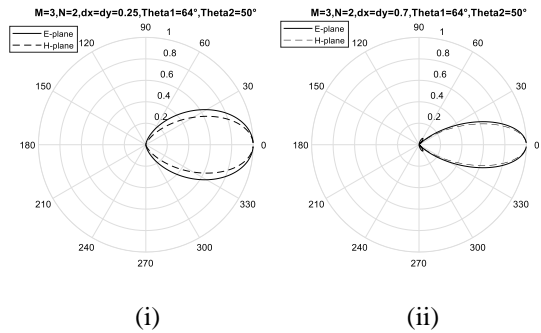


Figure 14: Radiation pattern of two-dimensional array in E & H planes when (i) $dx=dy=0.25$ & (ii) $dx=dy=0.7$

The directivity at different values of dx and dy is computed and presented in Table 2.

Table 2: The directivity.

$dx=dy$	0.25	0.3	0.4	0.5	0.6	0.7
D_0 (dB)	10.43	11.86	12.71	13.12	13.32	15.35

From the previous results, the performance of proposed antenna in terms of width and length patch (b & a), number of elements along the x-axis (M), number of elements along the y-axis (N), the spacing between the elements (dx & dy), directivity, distribution and radiation pattern was deeply studied. The parameters of the optimized antenna design that give a tradeoff between the performance and antenna size are shown in Figure 15.

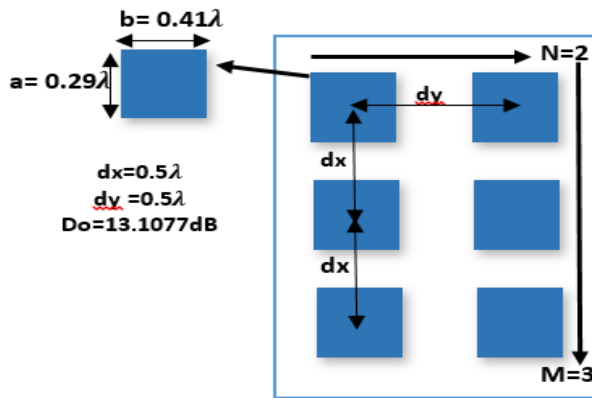


Figure 15: Proposed antenna design.

The antenna radiated signal must trace the satellite because the satellite moves in terms of personal mobile. Therefore, adaptive techniques were used to steer the main beam and decline the noise paths as presented in section 2.4. The Figure 16 shows steering the main beam in the desired direction and null in interference path for linear array.

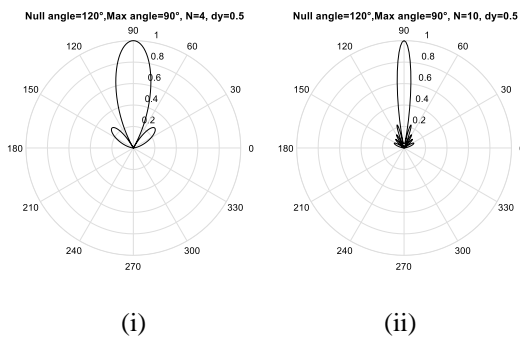


Figure 16: Steering the main beam at 90°, and null value at 120° for linear array with (i) N= 4, and (ii)=10.

Finally, the adaptive techniques were applied on the proposed planner array as presented in section 2.4. 3-D radiation pattern of the proposed planner array was computed and plotted as illustrated in Figure 17 and Figure 18.

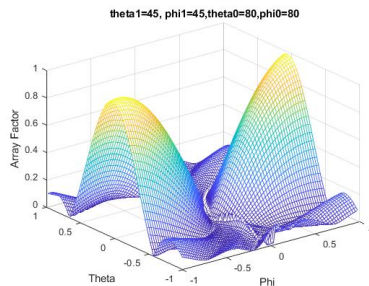


Figure 17: 3-D radiation pattern of the proposed planner array with adaptive steering technique.

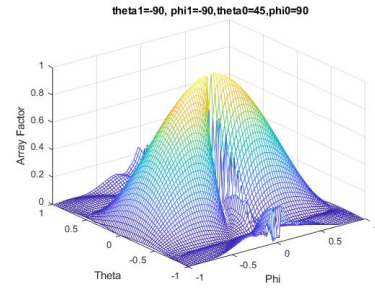


Figure 18: 3-D radiation pattern of the proposed planner array with adaptive steering technique.

4 Discussion

The Figures (6) and (7) show that the width 'b' and length 'a' have significant effect on the radiation pattern of the antenna. It can be seen that with an increase in 'b' as shown in Figure (6) (i) and (ii), the main beam width decreases noticeably in H-plane. This means that the radiation pattern in H-plane is significantly influenced by the width 'b', and no noticeable effect by the length 'a' as predicted from Eq. (3). However, with an increase in the length 'a' the main beam width decreases in E-plane as illustrated in Figure (7) (i) and (ii). The width 'b' has no noticeable effect on E-plane radiation pattern as proved from Eq. (2).

Figures (8-10) show that the spacing between the elements (dx & dy) have significant effect on the array factor of the planner antenna. It can be seen that as dx and dy decrease, the main beam width increases. However, as dx and dy increase, there will be more than one main beam with less width for each. As dx, dy increase more, the main beam width decreases, and more side lobes appear. Also, it can be noticed that, as elements number increases, the directivity increases as illustrated in Figures 11-13.

The Figure 14 shows that, as the distance between elements decreases, the main beam width increases in H-plane. Also, the distance affects the radiation pattern in E-plane significantly. As the elements distance increases the directivity increases accordingly. i.e., increasing the width of main beam. With a decrease in distance, the main beam width decreases and hence directivity decreases.

It is obvious that the directivity increases as the distance between the element increases and the elements number increase as well. However, practically, the antenna size is considered into account when the final design is proposed as shown in Figure 15. The performance of the proposed antenna with applying the adaptive techniques archives great steering and directivity, thus, it can be recommended for satellite mobile communication at a high satellite orbit.

5 Conclusion

This paper sets out to investigate the use of adaptive smart antennas in personal - satellite communications Link. It was found that, as the orbital radius increases the required number of satellites decreases accordingly, but the loss increases. This leads to weakness in the signal intensity. This discrepancy between the number of satellites and free space loss was overcome by means of designing a high gain antenna, hence increasing SINR. High gain adaptive planar microstrip patch antennas were proposed and simulated using MATLAB and the desired level of optimization was obtained to compensate the attenuation of signal intensity without increasing the transmitted power. The proposed adaptive antenna was able to steer the narrow main beam width towards the satellite with a directivity of 13.12 dB, and a null value towards interference directions to increase the signal to noise ratio. It was concluded that the software results that were obtained matched the theoretically predicted results. It was demonstrated that, the directivity increases as dx and dy increase, but on the other hand at the expense of the final antenna dimensions.

References

- Abo-Zeed, M., Din, J., Shayea, I., & Ergen, M. (2019). Survey on Land Mobile Satellite System: Challenges and Future Research Trends. *IEEE Access*, PP, 1-1. doi:10.1109/ACCESS.2019.2941900
- Behera, S. K. (2007). Novel Tuned Rectangular Patch Antenna as a Load for Phase Power Combining.
- Chrisman, B. P. (1989). *Planar Array Antenna Design Analysis*. Volume 1. Retrieved from
- Garg, R. (2001). *Microstrip antenna design handbook*. Boston, MA: Artech House.
- Karaliopoulos, M. S., & Pavlidou, F.-N. (1999). Modelling the land mobile satellite channel: a review. *Electronics & Communication Engineering Journal*, 11(5), 235-248. Retrieved from https://digital-library.theiet.org/content/journals/10.1049/ecej_19990506
- Kasabegoudar, V. G., & Kumar, A. (2013). Dual band coplanar capacitive coupled microstrip antennas with and without air gap for wireless applications. *Progress In Electromagnetics Research C*, 36, 105+.
- Khan, M. R. R., & Tuzlukov, V. (2010, 16-18 Oct. 2010). Beamforming for rejection of co-channels interference in an OFDM system. Paper presented at the 2010 3rd International Congress on Image and Signal Processing.
- Luo, Q., & Gao, S. (2014). Smart Antennas for Satellite Communications. In Z. N. Chen (Ed.), *Handbook of Antenna Technologies* (pp. 1-32). Singapore: Springer Singapore.
- Rappaport, T. S. (2002). *Wireless communications : principles and practice* (2nd ed ed.). Upper Saddle River, N.J.: Prentice Hall PTR.
- Rodríguez-Osorio, R. M., & Natera, M. A. S. (2010). On the Use of Ground Antenna Arrays for Satellite Tracking: Architecture, Beamforming, Calibration and Measurements.
- Wu, D., & Li, Q. (2005, 5-5 Oct. 2005). A New Routing Algorithm of Two-tier LEO/MEO Mobile Satellite Communication Systems. Paper presented at the 2005 Asia-Pacific Conference on Communications.
- Yang, S., Huang, C., & Hong, C. (2014). Design and Analysis of Microstrip Antenna Arrays in Composite Laminated Substrates. *Journal of Electromagnetic Analysis and Applications*, 6(06), 115.